Towards a Practical Single Element Null Steering Antenna

Yu-Hsuan Chen, Fabian Rothmaier, *Stanford University*
Dennis Akos, *University of Colorado at Boulder*
Sherman Lo and Per Enge, *Stanford University*

BIOGRAPHIES

Yu-Hsuan Chen is a research engineer at the Stanford GPS Laboratory. He received his Ph.D. in Electrical Engineering from National Cheng Kung University, Taiwan in 2011.

Fabian Rothmaier is a M. Sc. student in the Stanford GPS Research Laboratory. Before going to Stanford, he received his B. Eng. degree in Aviation System Management and Engineering at the University of Applied Sciences Bremen, Germany in 2015. Concurrently, he completed the Airline Pilot Flight Training at Lufthansa AG in Bremen, Germany and Phoenix, AZ. He is the current President of the Stanford Aviators club and a 2016 fellow of the International Society of Transport Aircraft Training (ISTAT). He has a German and US private pilot license and a commercial drone pilot certificate.

Dennis Akos obtained the Ph.D. degree from Ohio University in 1997. He is an associate professor with the Aerospace Engineering Science Department at University of Colorado at Boulder with visiting appointments at Stanford University.

Sherman Lo is currently a senior research engineer at the Stanford GPS Laboratory. He received the Ph.D. in Aeronautics and Astronautics from Stanford University in 2002.

Per Enge is a professor of Aeronautics and Astronautics at Stanford University, where he is the Vance D. and Arlene C. Coffman Professor in the School of Engineering. He directs the Stanford GPS Laboratory, which develops satellite navigation systems. He has been involved in the development of the Federal Aviation Administration's GPS Wide Area Augmentation System (WAAS) and Local Area Augmentation System (LAAS).

ABSTRACT

The GNSS signal properties which make it successful also make it vulnerable. Being an open signal transmitted from distant satellites allows it to be easily adopted and used worldwide. However, it also means that it is easy to interfere with or spoof. In the literature, antenna arrays or numerous receiver-based techniques have been proposed to detect and mitigate the interference. But, these approaches usually have complicated architectures and require significant additions or changes to the existing hardware. This makes these solutions difficult to adopt for safety of life applications. In previous work, a single element, dual feed antenna was designed to be capable of sensing the general direction of signal source. Its capabilities can then be used for spoof detection as well as interference mitigation. For instance, in aviation, the terrestrial interference sources usually originates from below the aircraft (i.e. the lower hemisphere). The single element dual feed antenna can distinguish signals from low and high elevations. Furthermore, it can then create a null toward the source direction to mitigate it. The antenna consists of a dual-feed patch, 90 degree hybrid coupler, variable phase shifter, power combiner, RF switches and microcontroller. Both right-hand and left-hand circular polarization signals (RHCP and LHCP, respectively) can be received by the dual feed patch. The body of aircraft extends the ground plane of antenna and alters the polarization of low elevation signals adjusting the RHCP and LHCP components. Hence, the body aids in discriminating high and low elevation sources. Null-steering is accomplished by combining the phase-shifted RHCP signal with the LHCP signal. The technology is adaptable to existing installations, replacing the antenna itself without changing the receiver or requiring additional antennas and their accompanying holes and cabling. Several iterations of components were constructed, tested and programmed to develop a miniaturized printed circuit board (PCB) version of the antenna with desired functionality. This paper describes the PCB design and implementation in detail. Several important modifications are made to solve potential issues on PCB and to improve performance. It also provides results of tests conducted to validate the miniaturized version of antenna. Results indicate that the antenna can clearly distinguish signals from different elevation and azimuth satellites.

INTRODUCTION

Our prior work [1], demonstrated the feasibility of our single element, dual feed antenna for anti-spoofing. This work utilized a prototype version of the antenna built using evaluation boards of various RF components. The work in this paper advances the antenna for use in real world applications with two major improvements. First, a printed circuit board (PCB) is designed and built to place the RF components. This miniaturization allows the antenna and its electronics to fit within a small form factor housing such that of a standard aircraft antenna. Moreover, modifications have been incorporated to improve and automate performance. These changes include replacing the analog phase shifter with an equivalent digital design and adding control logic to automate spoofing direction localization. The digital phase shifter simplifies the circuit design as the analog component requires a negative voltage supply as well as high voltage (15 volts). Also, the digital phase shifter is much smaller and easy to control. A u-blox GNSS receiver is added to provide the measurement to control logic. Originally, Dr. Emily McMilin advised to place smart bias-T for commutating with on-board GNSS receiver in [2]. This also reduces the size of antenna. For the PCB design, two matching networks are added to minimize the return loss from both feeds. The transmission lines from both feeds are laid out with equal electrical length to ensure equal electrical phase delay. The additional RF switches allows the antenna to more flexibly in changing to different modes. A state flow is programmed to switch between normal and anti-spoofing modes.

The paper is organized as follows. The first part describes the goal and basic technology of the dual feed patch as applied to spoofing detection and mitigation. The body of the paper describes the improved PCB design. It also details the preliminary test conducted to evaluate the elevation and azimuth discrimination of antenna.

DESIGN CRITERIA

The goal of the development is to build an antenna suitable for aviation with spoofing detection/mitigation features that could be an easy replacement for an existing antenna. The antenna applique is shown in Figure 1 which shows its major components connection and how it fits within the existing receiver installation. The antenna must be capable of operating in normal situation as a typical GNSS antenna while also being able to detect spoofing. Hence, it must have a switching mechanism in order to switch the antenna between normal and anti-spoofing modes. As the ideal solution would be to replace the currently installed antenna with the developed one without requiring any additional control and modifications to the existing receiver interaction, the mechanism should not require any feedback from the installed avionics. So the spoofing detection system is implemented completely within the antenna and its housing, not in the installed receiver (i.e. the on board receiver or avionics). The antenna is powered by the same coaxial cable accompanied with antenna output. Size is also an important consideration and it should follow aviation standards. ARINC standard 743 document states that the maximum size aviation form-factor antenna is 11.938 cm x 7.62 cm x 1.854 cm [3].

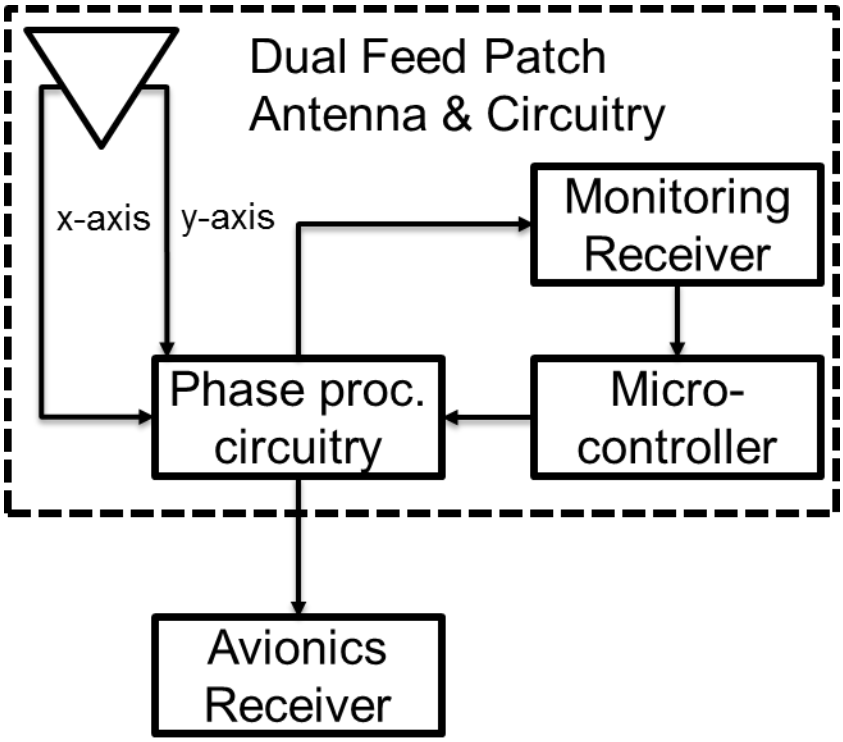

Figure 1. Overall dual feed patch concept of integration for existing avionics receivers

Mode	Output to Avionics Receiver	Output to Monitoring (u-blox) Receiver	Operations
Normal	RHCP	LHCP	spoof/jam detection
Anti-Spoofing	Composite signal	Composite signal	spoof/jam mitigation

SPOOF DETECTION & NULL STEERING

A dual-feed antenna can receive signals from the x-axis and y-axis based antenna body frame. The signals transmitted by GNSS satellites are right-hand circular polarized (RHCP). This results in the y-axis measured signal leading the x-axis signal by 90 degrees. A hybrid coupler is then used to combine the signals from the axes to form RHCP and LHCP signal components. The coupler is a four-port component consisting of two inputs and two outputs. X-axis and y-axis signals are connected to inputs and the coupler functions on those inputs by shifting one input by 90 degrees and adding it to the other. Depending on which input is shifted by 90 degrees, one gets either RHCP or LHCP. However, the relative phase between RHCP and LHCP signals is not aligned and depends on azimuth of satellite.

When mounted atop an aircraft, the body extends the ground plane of antenna and helps the detection of low elevation signal sources. A signal from the lower hemisphere must traversing the body of the aircraft. To conduct over the body surface, the signal must be essentially vertical polarized rather than circularly polarized, even if the transmitted signal was circularly polarized. This difference can be used to distinguish between a signal from above (satellite) and a signal from the ground (spoofer). Hence the antenna can provide spoof detection by testing if a signal has mostly RHCP (authentic) or if it has significant power in LHCP components (spoofing or multipath or low elevation satellite).

Furthermore, the antenna can null the spoofing or interfering signal. The basic concept for null-steering technique is to combine two type of signals received from the antenna using a phase-shifter and a combiner. A deep null is formed when we combine the LHCP and RHCP signal components provided they have 1) similar magnitude and 2) out-of-phase or 180 degree phase difference. To properly match magnitude, the gain pattern of antenna is investigated. The gain pattern of the dual-feed antenna was measured in a radio frequency enclosed structure and is shown in Figure 2. The solid and dash curves represent gain pattern for RHCP and LHCP, respectively. The polar axis indicates the elevation of satellite. The magnitude is shown in decibel (dB)

for received power. The gain difference between RHCP and LHCP is defined as Cross Polarization Discrimination (XPD)[2]. For high elevations (> 60 degrees), the 20 dB XPD is so significant that the null would not be deep. For low elevations (< 10 degree), the XPD is down to 5 dB or lower allows for a deep null.

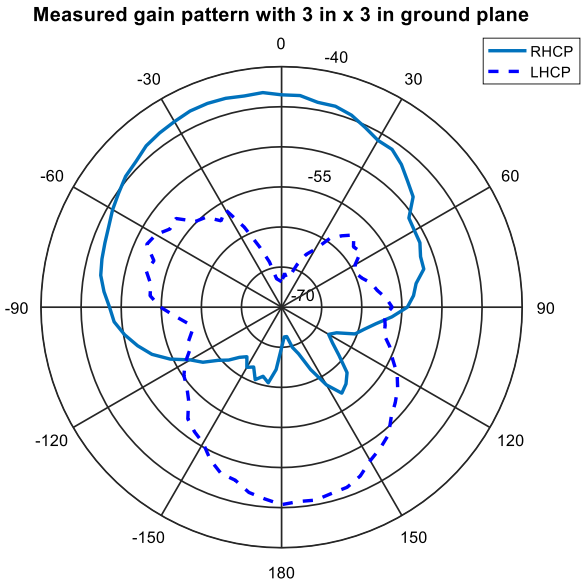

Figure 2. Gain pattern of dual-feed patch antenna

The generic resulted gain pattern in azimuth by combining RHCP and LHCP is illustrated in Figure 3. The gain pattern is symmetric respect to 0 to 180 degree azimuth line. There are two main lobes in 0º and 180º and two nulls in -90º and 90º. For searching for azimuthal null, phase shifter scan through 360º in order to find deep null in Carrier-to-Noise ratio (CNo). The scanning process is actually steering the null in the azimuth from 0º to 180º. It usually takes a few cycle to ensure the null appearing at the same azimuth angle. Relationship between phase shifter value, azimuthal null and CNo is shown in Figure 4. The depth of null in CNo is elevation dependent explained in the previous section. The null associated phase shifter value depends on antenna attitude and satellite azimuth.

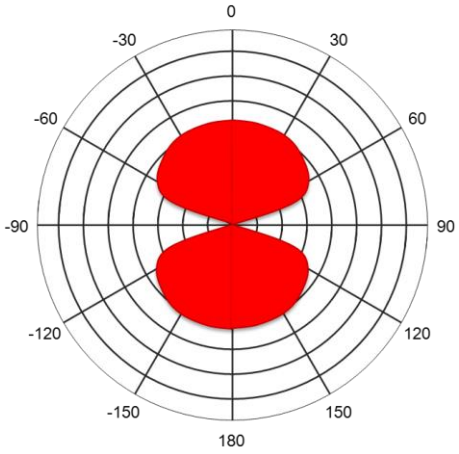

Figure 3. Illustrated gain pattern of combining RHCP and LHCP from dual-feed patch antenna

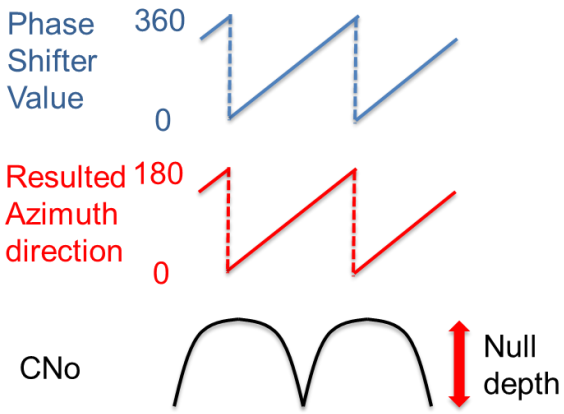

Figure 4. Relationship between phase shifter value, azimuthal null direction and CNo

ANTENNA DESIGN

The antenna is designed with size 3 inch x 3 inch or 7.62 cm x 7.62 cm which fits the standard for an aviation antenna. It is designed on a four layer printed circuit board (PCB). Minimum trace is 6 mil (.001 inch) and minimum hole dimension is 10 mil. The dual feed patch antenna is placed on the top layer. Most of top layer is metal used for constructing a complete ground plane. The second layer is power or Vcc. The third layer is ground for constructing transmission lines with the bottom layer. All the components are placed on the bottom layer. Among them, radio frequency (RF) parts are connected by 50 ohm transmission lines. The antenna has one antenna output for powering and connecting to an avionic receiver. There are some additional U.FL connectors and pin headers for debugging purpose. The block diagram of antenna is depicted in Figure 5. The dual feed patch antenna receives signals from both x and y axes. There are matching networks after both feeds to ensure the impedance matching to 50 ohm. Two low noise amplifiers (LNA) with 20 dB gain are placed right after matching network to amplify the receiving power. This helps lower the overall noise figure by having the high gain LNA in the first stage. Two transmission lines from both feeds to LNAs are designed with equal length to ensure equal electrical phase delay between two traces. It is important that the phase difference between x and y axis signals arriving to the hybrid coupler is kept the same as found at the feed points as any phase error would contribute to errors in forming the RHCP and LHCP signals. The amplified x and y axis signals are then fed into the hybrid coupler. The coupler combines these and outputs the RHCP and LHCP signal components. For debugging purposes, a double-pole, double-throw (DPDT) switch is inserted to switch the output path between RHCP and LHCP components. This is useful for checking signal power for both signals. The two signals are then fed into another double-pole, three-throw (DP3T) switch which is used to switch between normal and anti-spoofing modes. For normal mode, the RHCP signal is directed to antenna output and LHCP signal is directed to the u-blox GNSS receiver. For anti-spoofing mode, the RHCP signal goes through a variable phase shifter which is controlled digitally by the microcontroller unit (MCU). The phase shifter has 8 bits (256 steps) resolution for whole 360 degrees resulting in 1.4 degrees for each step. A finer resolution phase shifter generally creates deeper nulls. The phase shifter also causes the RHCP signal to be attenuated by 6dB. To equalize the power difference, the LHCP is also attenuated by 6 dB using an attenuator. The phase-shifted RHCP is combined with attenuated LHCP by a power combiner. The composite signal is then split to two ways. One goes to antenna output, the other goes to the u-blox receiver. The antenna output is switched between the RHCP and composite signal which provides the avionics receiver with the unadulterated and the spoof mitigated signals, respectively. The input of u-blox receiver is switched between LHCP (normal mode) and composite signal (anti-spoofing mode). The former allows for spoof detection while the latter is used for spoof mitigation. A microcontroller unit (MCU) communicates with u-blox receiver to obtain the CNo and position information. This information is used for determining the antenna operational modes and controlling all the switches. For example, if the spoof detection mode indicates spoofing, then the MCU will switch to anti-spoofing mode. The switching and operational flow is described in detail in the next section. Photo of PCB is shown in Figure 6.

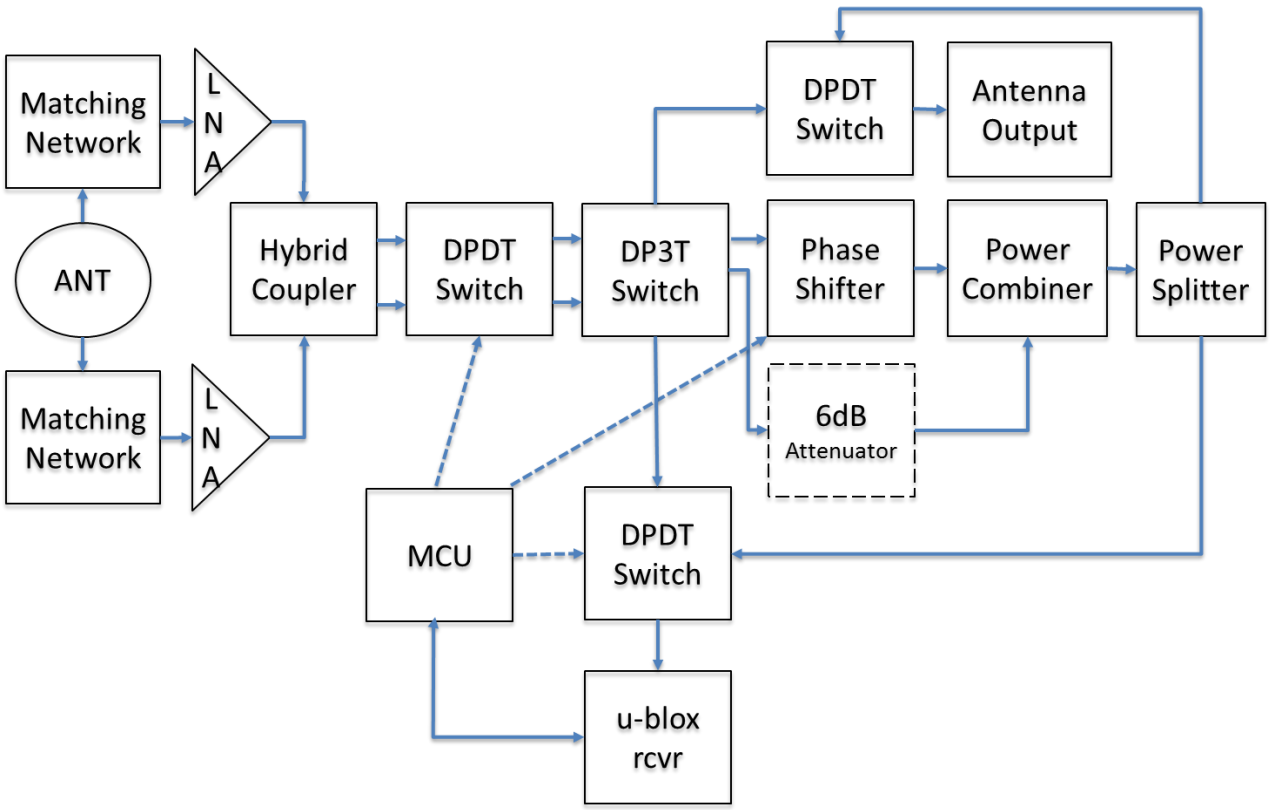

Figure 5. Block diagram of the major components of the antenna

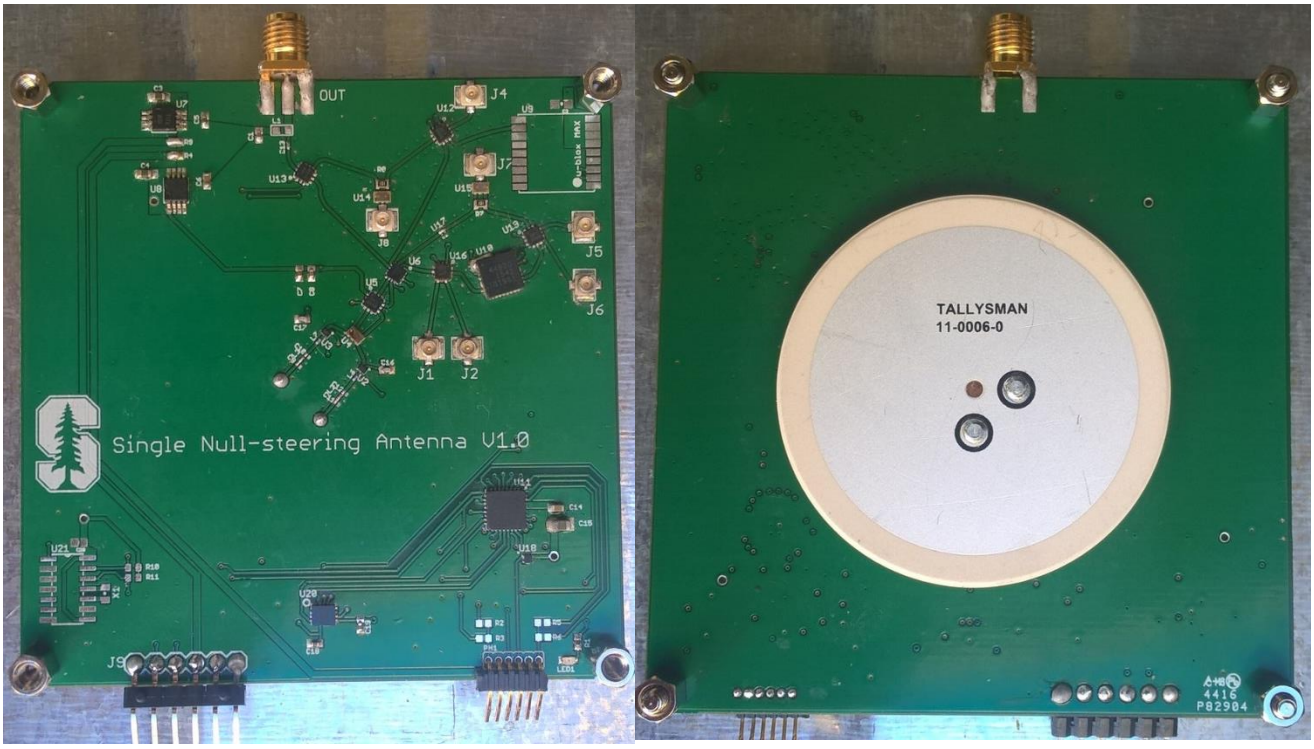

Figure 6. PCB of antenna

OPERATIONAL FLOW

The operational flow of antenna describes the operational modes and associated output signals. The flow is shown in Figure 7. Initially, the antenna is in normal mode and outputs the RHCP signal to the avionics receiver. It also directs the LHCP signal to the u-blox receiver and its CNo is assessed to determine whether it is higher than a predetermined threshold. Another spoof detector implemented is Automatic Gain Control (AGC), as described in [4].

The threshold is set to assess if the spoofing signal is coming from lower hemisphere, meaning if the LHCP signal has a higher CNo than the threshold. The threshold is calculated by modeling the distribution of LHCP CNo from the nominal GNSS signal and selecting a probability of false alarm (Pfa). Once is LHCP CNo is higher than the threshold, the DP3T is switched and a 360 degree scan is initiated by changing the phase in phase shifter. The scanning should be run for a few cycles to ensure that the deep null appears in the specified direction. If deep nulls are found from several different satellites for a specific direction, this indicates that the null has been steered in the direction of a potential spoofer. After finding the spoofer direction, the MCU fixes the phase shift to the direction determined and then enters the anti-spoofing mode. In the anti-spoofing mode, the antenna outputs the composite signal in the null steered or spoofing direction. The same composite signal is still examined using CNo. If the antenna attitude changes, the u-blox receiver CNo outputs can be used to determine the new direction of the spoofing signal. For extended duration such as a few minutes (T), the antenna could return to normal mode to check if the spoofing signal has disappeared.

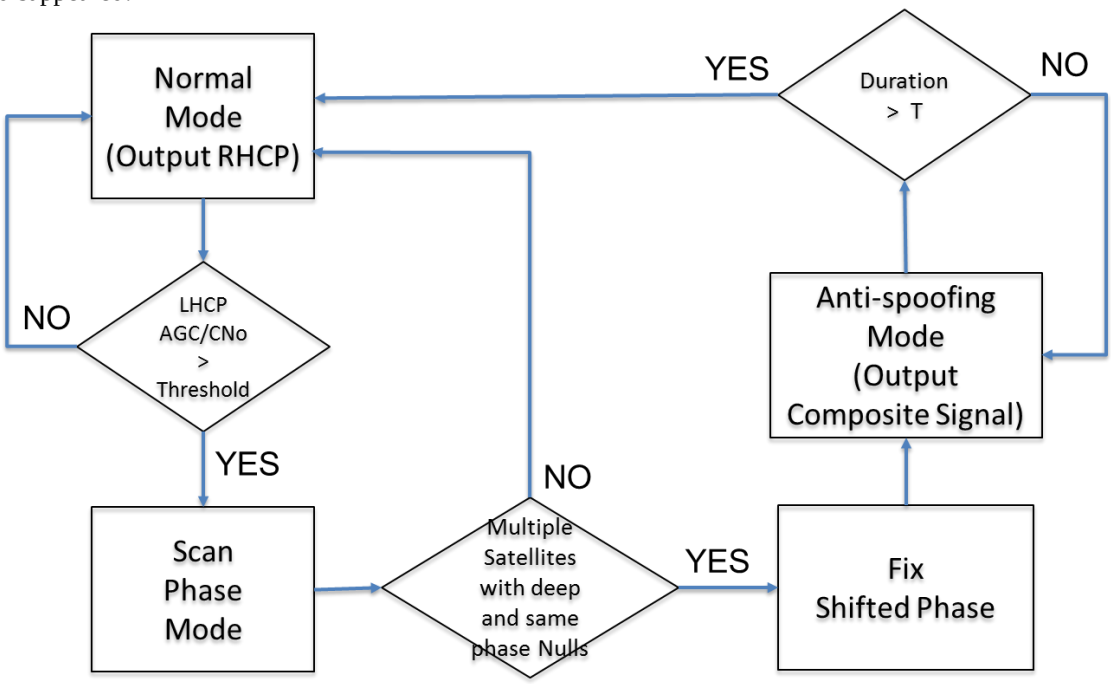

Figure 7. Logic flow of the operations of the antenna

ANTENNA TESTING

The antenna is mounted on a metal cylindrical body to simulating the body of aircraft. The rooftop of the Durand building at Stanford University is used as an initial test site and this is shown in Figure 8.As the broadcast of any signal on L band is illegal, the antenna is currently tested without any spoofing signals. Instead, the on-air satellite signal from different elevations and elevations can used to initially test and evaluate antenna's nulling effect. As explained in the null-steering section, the lower elevation satellite is, the deeper the null will result. So testing on the roof of a four story building allows us to potentially receive satellite signals from the horizon or below. To make the test more realistic, it is desirable to have strong "spoofing" signals. To enhance the null performance, the 6 dB attenuator on LHCP before power combiner is removed. In this case, the RHCP is attenuated 6 dB by phase shifter and LHCP has no attenuation. That decreases the power difference between RHCP and LHCP signals resulting in a deeper null as potentially the expense of less discrimination. During the test, the phase shifter is programmed to change 1.4 degree phase every 0.2 seconds. The entire 360 degree cycle thus takes 51.2 seconds. The first test

was conducted on December 1, 2016. CNo from different satellites are collected for 10 minutes allowing for 12 complete cycles. The sky plot of satellites in view is shown on the left of Figure 9. The elevation angle profile over time of GPS satellites, PRN 14 and PRN 3, is shown on the right side of Figure 9. It shows that the two satellites have elevation angles of roughly 80 and 13 degrees, respectively, at the time of the test. The test results are shown in Figure 10. The CNo over time for both satellites have 12 ripples corresponding to 12 complete cycles of the phase shifting. One can see the antenna beam and null steering. For high elevation (80 degree) GPS PRN 14, the difference of highest and lowest CNo is 10 dB. For low elevation (13 degree) GPS PRN 3, the difference is 30 dB. The results validates the ability of the antenna to distinguish the high and low elevation by comparing null depths.

Figure 8. Antenna test setup on the roof of the Durand building (about 60 feet above ground level)

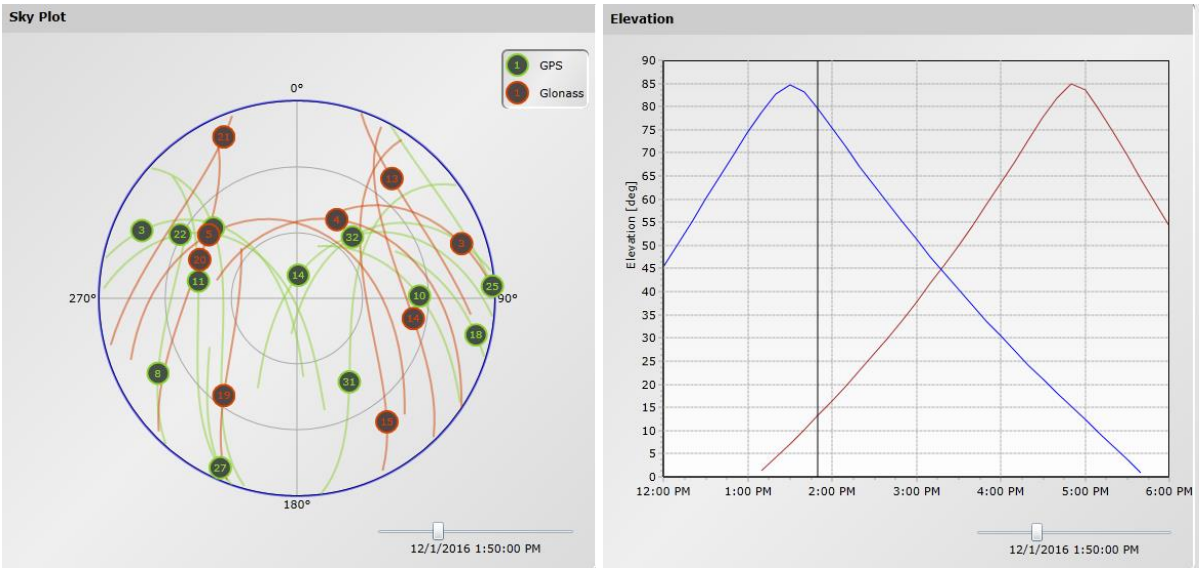

Figure 9. Left: sky plot; right: elevation with time, blue curve is GPS PRN 14 and red curve is GPS PRN 3
Courtesy of Trimble's GNSS planning online tool

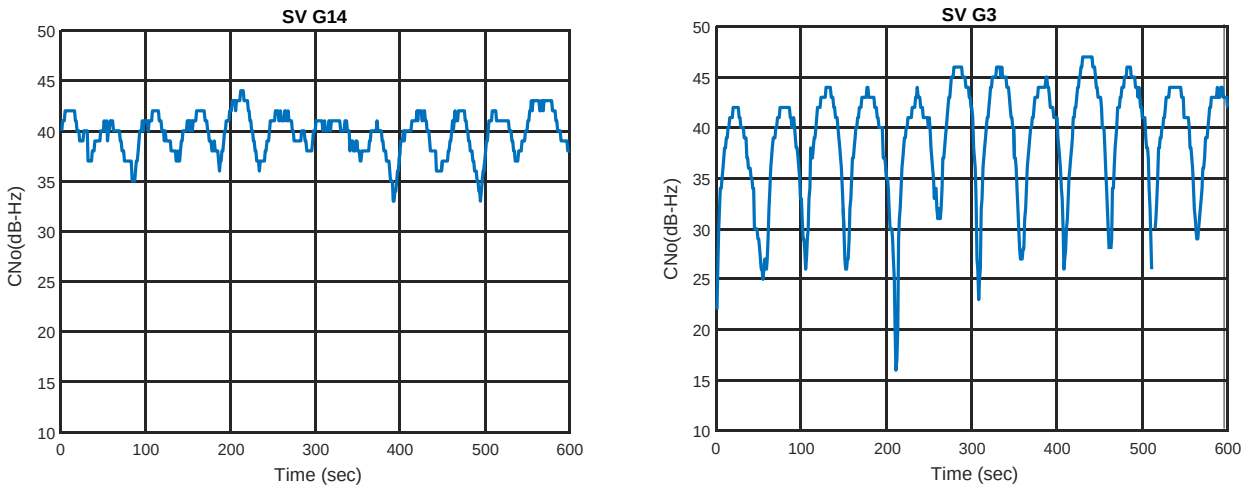

Figure 10. CNo with time left: GPS PRN 14 at 80 degree elevation, right: GPS PRN 3 at 13 degree elevation

The second test was conducted on January 13, 2017 for six-hour long data collection. In this six-hour period, GPS PRN 3 moved from low elevation to high elevation. So, we can evaluate the antenna performance for all elevation angles. The results are shown in Figure 11 with two y axes plotted. CNo is in left axis and elevation is in the right axis. Again, this result is collected when 6 dB attenuation on LHCP is removed. The null depth in the normal set up case should be smaller. However, the trend reveals that CNo in lower elevation has deeper null. Null depth has around 5 dB when the elevation is higher than 60º and up to 25 dB in the elevation lower than 30º.

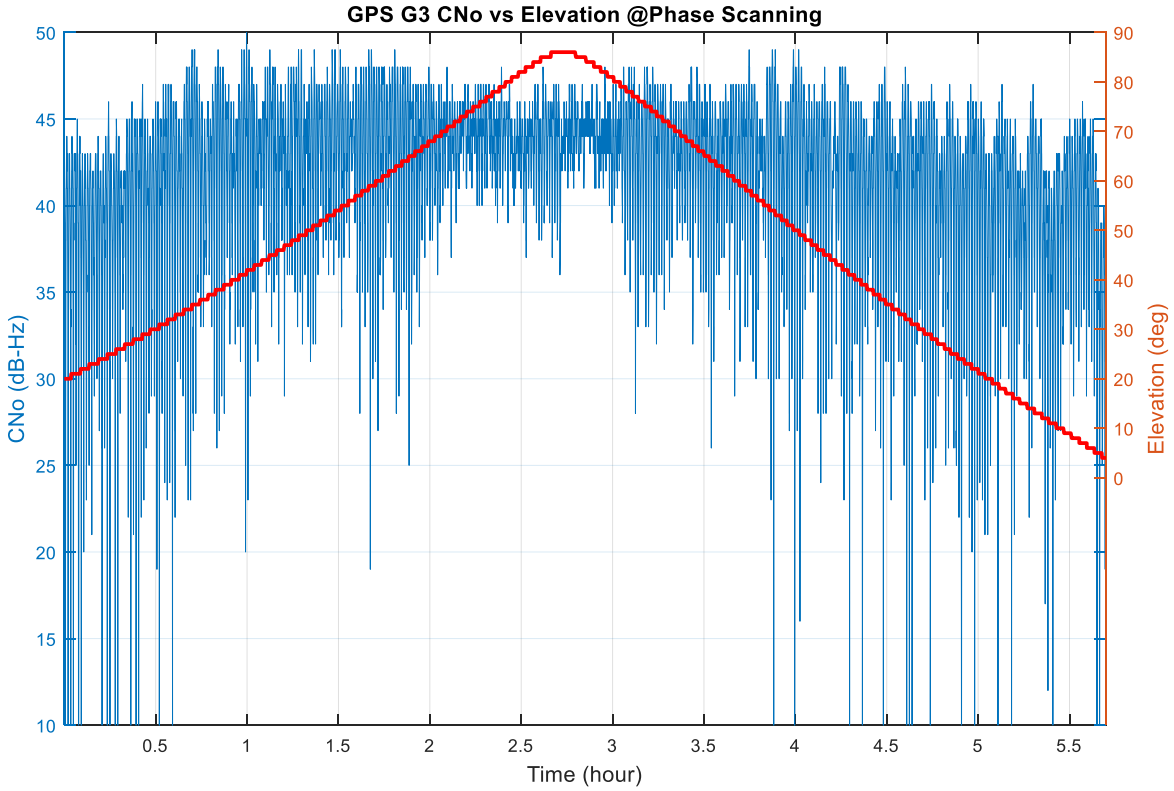

Figure 11. GPS PRN 3 CNo (left axis) and elevation (right axis) over time

For evaluating the azimuthal null, a 400-second time window is chosen when three satellites are in similar elevation. The sky plot is shown in Figure 12. Two of them, PRN 1 and 22, are in similar azimuth. The other satellite PRN 32 with 90º difference in azimuth from the other two satellites. Figure 13 shows CNo with time left for all satellites. Because the phase scanning cycle time is 51.2 seconds, there are 8 cycles in the time windows. The peaks and nulls of PRN 1 and 22 appear roughly at the same time. However, peaks of PRN 32 appear when the nulls of the other two satellites do. This result can conclude the antenna can distinguish signal from different azimuth. It is noted that there is 180º ambiguity in azimuth due to symmetric gain pattern of combining RHCP and LHCP.

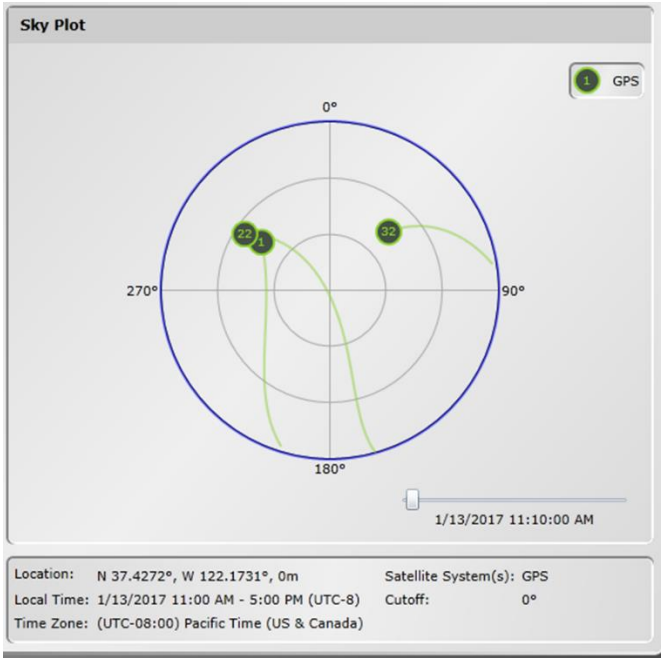

Figure 12. Sky plot of GPS PRN1/ PRN 22/ PRN32 when data collection

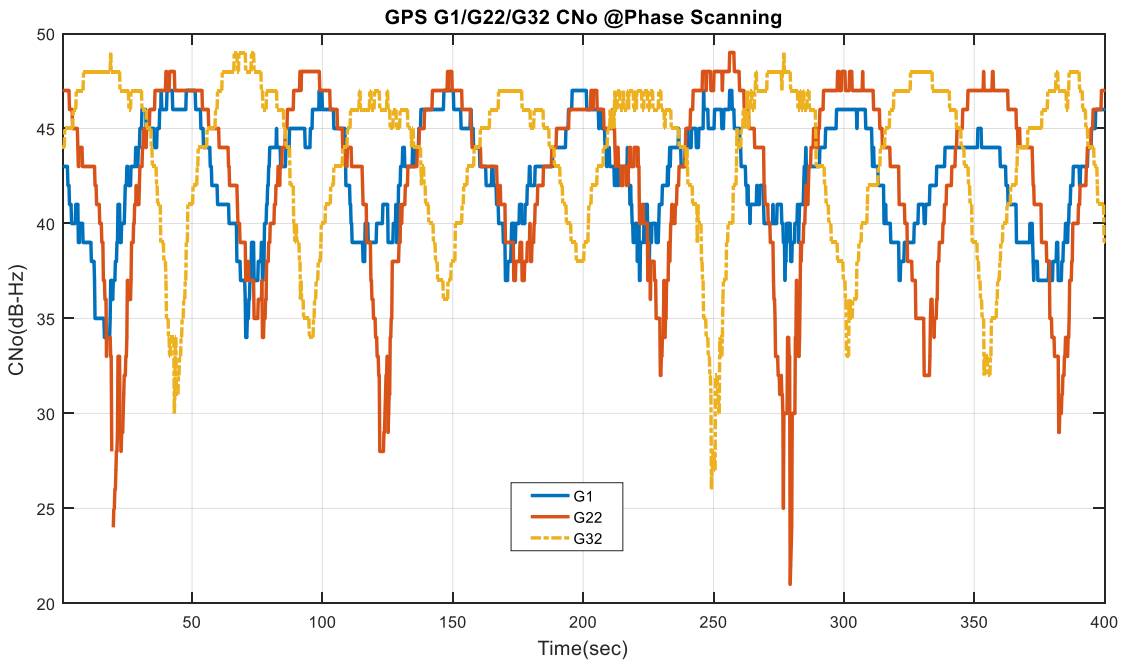

Figure 13. GPS PRN1/ PRN 22/ PRN32 CNo with time left

CONCLUSION AND FUTURE WORK

A dual-feed, single element, form-factored antenna is designed and implemented on a PCB and is tested with determination of angle of arrival capability. The resulting antenna can automatically detect and then mitigate a spoofing signal. The preliminary testing result shows the basic function of the antenna providing strong indication of a simulated spoofing signal (in the form of a low elevation satellite). The antenna can distinguish signal from high or low elevation satellites and different azimuth satellites. Future work includes refining the PCB design and implementing the full proposed operational flow. We also plan to implement its anti-jamming functionality. Additional testing is planned with actual spoofing signals transmitted within an enclosed RF shielded chamber. We are also planning to test the antenna on an aircraft and to attend live jamming/spoofing events to further test/refine the antenna and its design.

ACKNOWLEDGMENTS

The authors gratefully acknowledge the support of the FAA and Stanford Center for Position, Navigation and Time. The authors acknowledge Dr. Emily McMilin for providing testing equipment and advice. The authors also acknowledge Adrien Perkins and Kazuma Gunning for assisting the tests.

REFERENCES

[1] McMilin, Emily, Chen, Yu-Hsuan, De Lorenzo, David S., Lo, Sherman, Akos, Dennis, Enge, Per, “Field Test Validation of Single-Element Antenna with Anti-Jam and Spoof Detection,” Proceedings of the 28th International Technical Meeting of The Satellite Division of the Institute of Navigation (ION GNSS+ 2015), Tampa, Florida, September 2015, pp. 3314-3324.

[2] McMilin, Emily, Single Antenna Null-Steering for GPS & GNSS Aerial Applications, Ph.D. Dissertation, Stanford University, March 2016

[3] Aeronautical Radio, Incorporated, ARINC 743B, May 2009

[4] Akos, Dennis M., "Who's Afraid of the Spoofer? GPS/GNSS Spoofing Detection via Automatic Gain Control (AGC)", *NAVIGATION, Journal of The Institute of Navigation*, Vol. 59, No. 4, Winter 2012, pp. 281-290.